Metamaterials for the Terahertz Spectral Range

Ing. Filip Dominec

Advisor: Dr. Mgr. Filip Kadlec (Fyzikální ústav AVČR)
Consultant: doc. Dr. Ing. Ivan Richter (FJFI ČVUT)

Opponents: doc. Ing. Lukáš Jelínek, Ph.D.,
and doc. Dr. Mgr. Kamil Postava (VŠB-TU Ostrava)

Ph. D. Dissertation Defence
13th December 2016

Thesis goals in short

1. Elaborate an accessible theoretical background describing the **electrodynamics of periodic structures**
2. Emphasize the importance of taking the **nonlocal medium response** into account
3. Examine, in particular, structures lying **at the boundary** between the metamaterial and photonic crystal paradigms
4. Experimentally validate part of the numerical results, and **compose an overview** of periodic structures behaviour
5. Ensure that all developed simulation scripts are **published online**

What are metamaterials?

Proposed definition of a metamaterial

A metamaterial is any inhomogeneous structure with behaviour determined more by its shape than by constituent materials, that we attempt to describe as a homogeneous one

More usually, metamaterials are defined as periodic structures artificially designed to achieve some values of *effective parameters* that are not found in natural materials.

Large part of metamaterial research is aimed at achieving *negative effective index of refraction* $N'_{\text{eff}} < 0$, which is expected to occur if simultaneously the effective permittivity $\varepsilon'_{\text{eff}} < 0$ and permeability $\mu'_{\text{eff}} < 0$ are negative.

(a) Wickersham (1960)

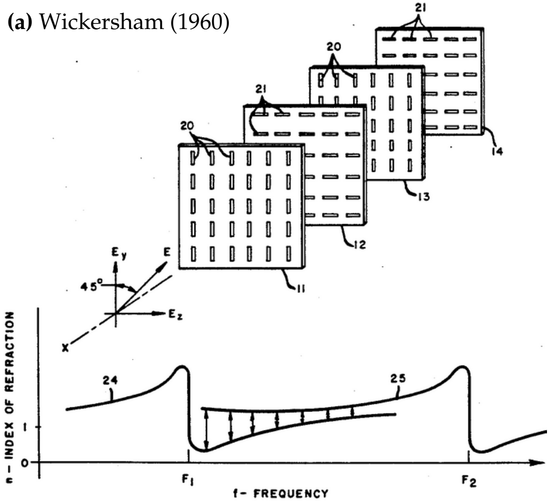

(b) Anderson (1967)

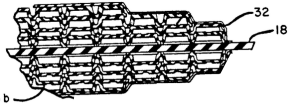

(c) Hannan (1966)

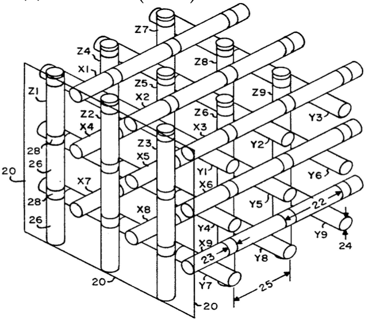

J. A. F. Wickersham. Artificial dielectric polarizer. US Patent 2,921,312. 1960. URL : http://www.google.com/patents/US2921312.
D. L. Anderson. Artificial dielectric lens structure. US Patent 3,329,958. 1967. URL : http://google.ru/patents/US3329958.
P. W. Hannan. Artificial dielectric using interspersed rods. US Patent 3,254,345. 1966. URL :
http://www.google.com.py/patents/US3254345.

Early photonic crystals

Photonic crystals (PhC) are periodic structures aimed at engineering the photonic band gap and density of states. Their effective parameters are usually not determined.

(a) Ho (1994)

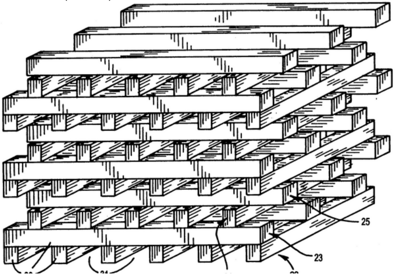

(b) Sweatt (2005)

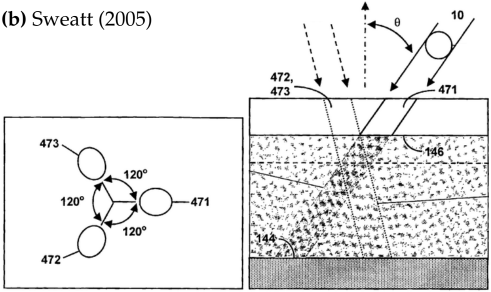

E. Yablonovitch. Inhibited Spontaneous Emission in Solid-State Physics and Electronics. Phys. Rev. Lett. 58, 2059–2062 20(1987).
K. Ho, C. Chan, and C. Soukoulis. Periodic dielectric structure for production of photonic band gap and devices incorporating the same. US Patent 5,335,240. 1994. URL : https://www.google.com.ar/patents/US5335240.
W. Sweatt and T. Christenson. Method for the fabrication of three-dimensional microstructures by deep X-ray lithography. US Patent 6,875,544. 2005. URL : https://www.google.com.ar/patents/US6875544.

2000’s: Merging of MM and PhC paradigms?

Two paradigms of *metamaterials* (MM), which were earlier denoted as *artificial dielectrics*, and *photonic crystals* (PhC) developed separately over few decades.

Waves in periodic structures vs. in natural media

Light in MMs	$\leftrightarrow$	$\lambda \gg a$	$\leftrightarrow$	Light in a crystal
Light in PhCs	$\leftrightarrow$	$\lambda \sim a$	$\leftrightarrow$	Electron wave in a crystal

However, as the metamaterial research approaches the optical frequencies, the $\lambda \gg a$ limit can not be held.

The metamaterial assumption $\lambda_0 \gg a$ is unsustainable

…for majority of realistic NIR/optical metamaterials

Table: Short survey for the ratio of free-space wavelength λ_0 to the unit-cell size (parallel and perpendicular to **k**) in selected publications

Source	λ_0 (nm)	$\lambda_0/a_{\|\|}$	$\lambda_0/a_{\perp}$	type
Šindler et al. 2016	350000	6–10	6–10	Mie
Zhang et al. 2005	1300	7	**2.2**	SRR
Dolling et al. 2007	780	8	**2.6**	fishnet
Gong et al. 2014	565	8	**2.4**	fishnet
Aslam et al. 2012	510	14	**2.1**	fishnet
Xu et al. 2013	365	**2.4**	–	2-D layers

We must carefully review all approaches to MMs that assume that the unit cells a are *just small*; in practice, they are not.

Šindler, M., et al., Optics Express, 24(16), 18340-18345, (2016); Zhang, S. et al., Phys. Rev. Lett., 94(3), 037402 (2005).
Dolling et al. Opt. Lett. 32, 53–55 (2007); Gong, B., et al.,. Sci. Rep., 4 (2014).
Aslam, M. I., and Güney, D. Ö. JOSA B, 29(10), 2839-2847 (2012).; Xu, T., et al., Nature, 497(7450), 470-474 (2013).

Dielectric rod array

...has been investigated first as a photonic crystal with a photonic band gap, and since 2000s also as a metamaterial with $N'_{\text{eff}} < 0$.

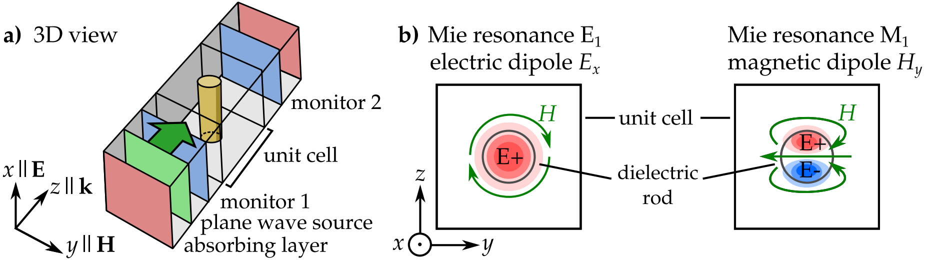

(a) Simulation layout for computation of $N_{\text{eff}}, Z_{\text{eff}}, \varepsilon_{\text{eff}}$ and μ_{eff} using the *scattering-parameters* method. Cells are periodic in the **x** and **y** directions. **(b)** Cross-sections through the **y-z** plane showing two resonant modes. The dielectric permittivity at $f = 1$ THz was 89.5 + 0.23i, corresponding to polycrystalline titanium dioxide.

W. B. Weir. Proc. IEEE 62, 33–36 (1974); A. Nicolson and G. Ross. Instrum. Meas., IEEE Transactions on, 19, 377–382 (1970).

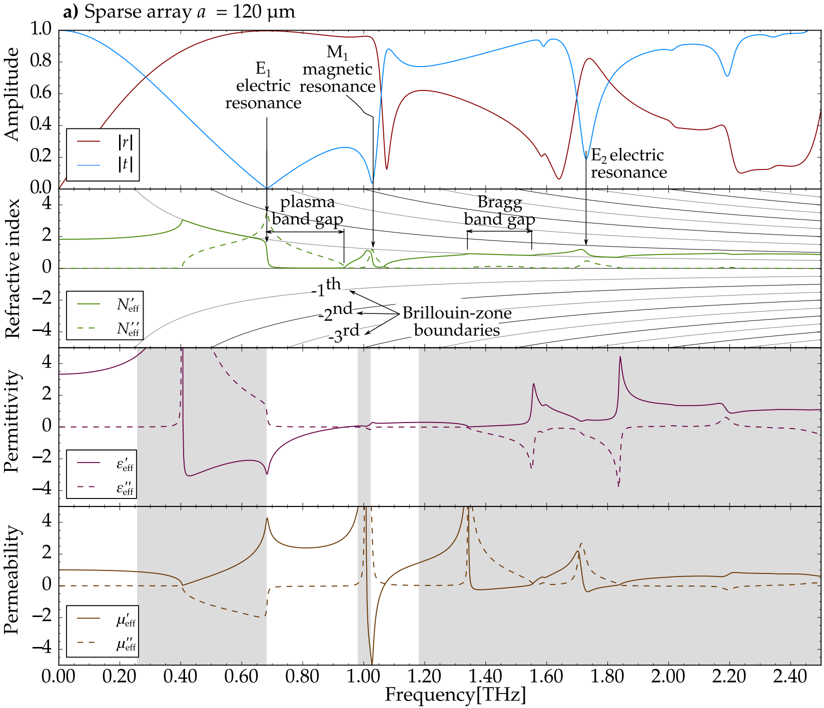

a) Sparse array a = 120 μm
Amplitude
Refractive index
Permittivity
Permeability
Frequency[THz]
|r|
|t|
E1 electric resonance
M1 magnetic resonance
E2 electric resonance
plasma band gap
Bragg band gap
-1th
-2nd
-3rd
Brillouin-zone boundaries
N′eff
N′′eff
ε′eff
ε′′eff
μ′eff
μ′′eff

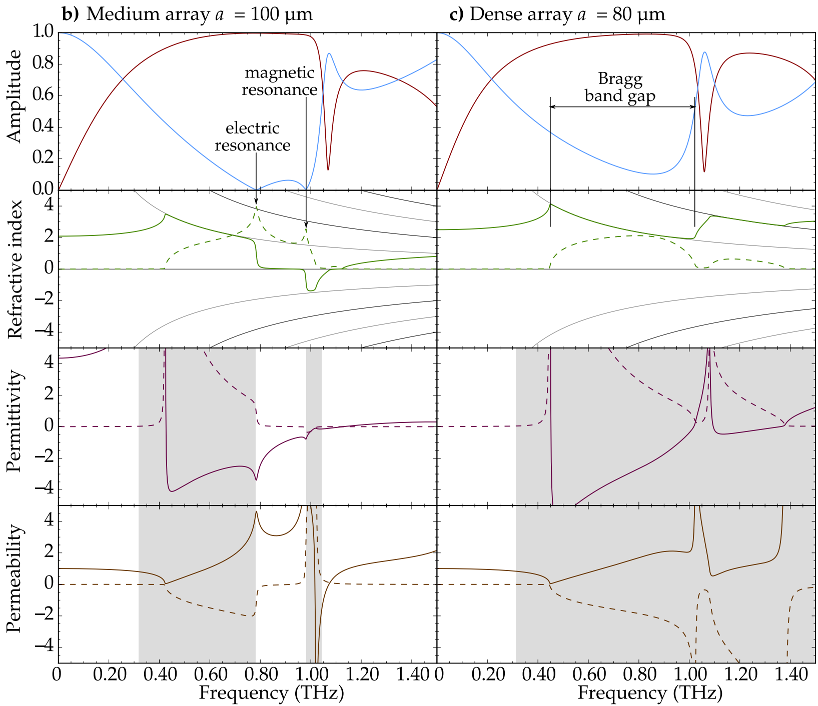
b) Medium array a = 100 µm
c) Dense array a = 80 µm
Amplitude
magnetic resonance
electric resonance
Bragg band gap
Refractive index
Permittivity
Permeability
Frequency (THz)
Frequency (THz)
1.0
0.8
0.6
0.4
0.2
0.0
4
2
0
−2
−4
0
0.20
0.40
0.60
0.80
1.00
1.20
1.40

Color coding of refractive index

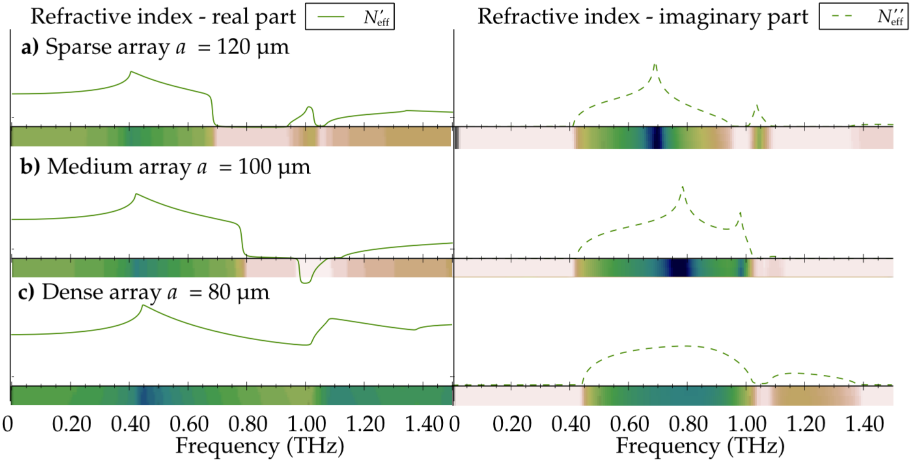

Spacing scan: $N'_{\mathbf{eff}}, N''_{\mathbf{eff}}$ for $\rho = 10$ µm, $\varepsilon_r = 100$

Real (N'_{eff}, left panel) and imaginary (N''_{eff}, right panel) parts of refractive indices

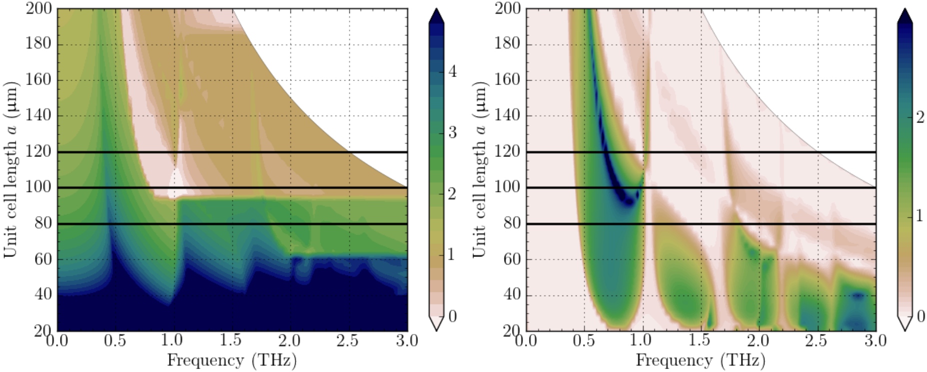

Dielectric rod array – sketch of spacing scan

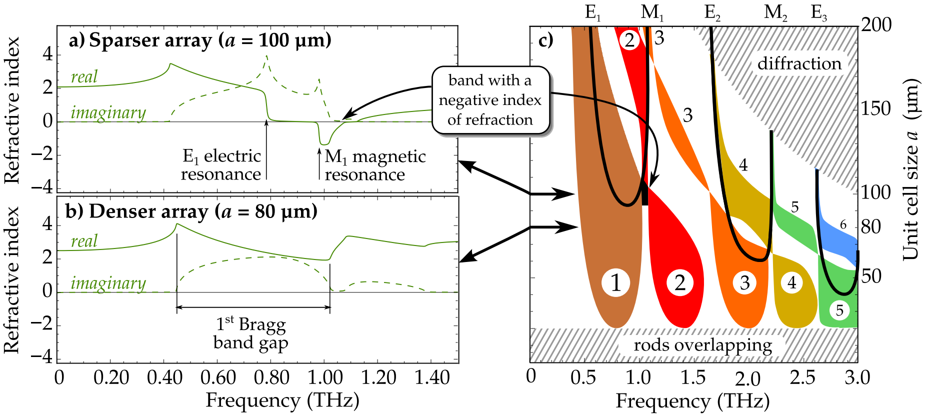

F. Dominec et al. Transition between metamaterial and photonic-crystal behavior in arrays of dielectric rods. Opt. Express 22, 30492–30503 (2014).
M. V. Rybin et al. Phase diagram for the transition from photonic crystals to dielectric metamaterials. arXiv:1507.08901 (2015).

Nonlocal response

The trouble with using $\varepsilon_{\text{eff}}(\omega)$ and $\mu_{\text{eff}}(\omega)$ is that they only describe the local response.

The medium may be *nonlocal*, i.e., elecric field in point $\mathbf{r}$ makes it develop polarisation also in surrounding points $\mathbf{r} \neq \mathbf{r}'$.

Waves in periodic structures vs. in natural media II.

Light in MMs	$\leftrightarrow$	$\lambda \gg a$	$\leftrightarrow$	Light in a crystal
Light in PhCs	$\leftrightarrow$	$\lambda \sim a$	$\leftrightarrow$	Electron wave in a crystal
Previous example	$\leftrightarrow$	$\boldsymbol{\lambda \lesssim a}$	$\leftrightarrow$	**Nonlocal medium!**

For a harmonic wave, nonlocality translates into *spatial dispersion*, and the effective parameters explicitly depend on the wave vector $\mathbf{k}$:

$$\varepsilon_r(\omega), \mu_r(\omega) \to \varepsilon_r(\omega, \mathbf{k}), \mu_r(\omega, \mathbf{k})$$

Current-driven homogenization

The customary approach involved selecting a frequency, measuring the scattering parameters (reflectance and transmittance) and computing the allowed wavenumbers.

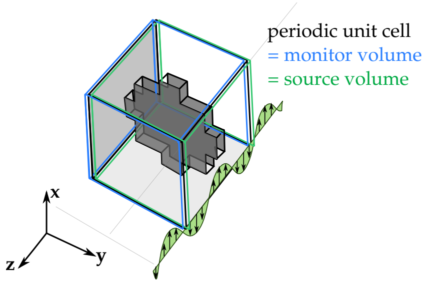

Instead, in the *current-driven homogenization*, the volumetric current source imparts a desired wavevector **K** to the whole unit cell, and looks for all corresponding resonance frequencies.

M. G. Silveirinha. Metamaterial homogenization approach with application to the characterization of microstructured composites with negative parameters. Phys. Rev. B 75, 115104 (2007).

C. Fietz and G. Shvets. Current-driven metamaterial homogenization. Physica B 405, 2930–2934 (2010).

Testing current-driven homogenization (CDH) on the rod array with $a = 100$ μm, $\rho = 10$ μm, $\varepsilon_r = 100 \rightarrow$

Bubbles are computed using CDH; the green dispersion curve shows the effective index of refraction from the scattering-parameters method as

$$K = \frac{2\pi N'_{\text{eff}} f}{c}.$$

Dashed part denotes negative values of N_{eff}

Result

This confirms that the use of scattering parameter method was appropriate for this rod array

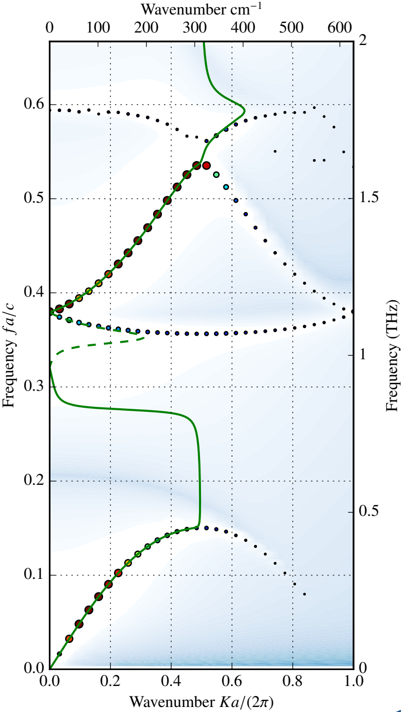

Electro-magnetic split-ring resonator

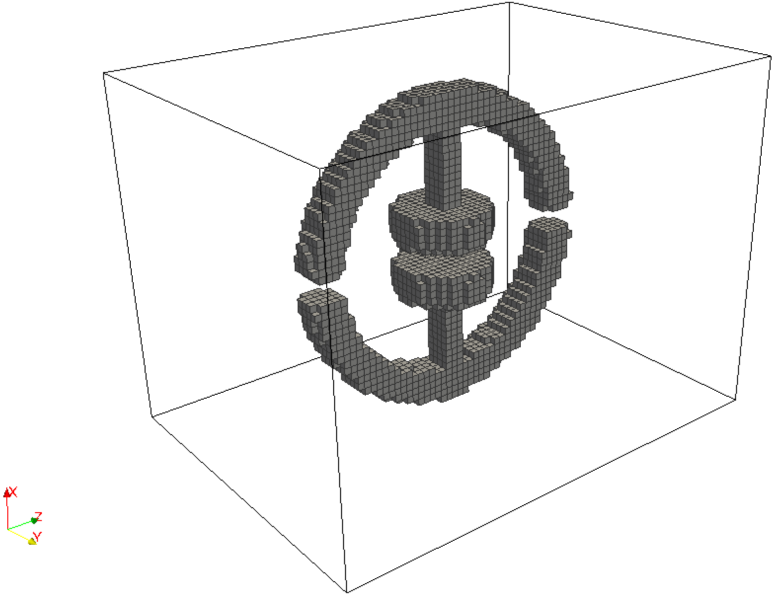

Electro-magnetic split-ring resonances

The structure exhibits two resonances; one with a magnetic dipole (left) the second with an electric one (right).

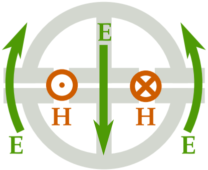

By changing the inner capacitor radius, we can tune the electric resonance frequency.

Other parameters will remain constant: capacitor splitting := 6 µm, outer ring radius := 45 µm, conductor cross-section := 10×10 µm and unit cell size := 100×100×100 µm.

Current-driven homogenization (CDH) of an electro-magnetic split-ring resonator

inner capacitor radius of $\boldsymbol{\rho_c} = \mathbf{6}$ μm →

Bubbles are computed using CDH; the green dispersion curve comes from the scattering-parameters method. Note that

$$K = \frac{2\pi n f}{c}$$

capacitor splitting = 6 μm,
outer ring radius = 45 μm,
conductor cross-section = 10×10 μm
unit cell size = 100×100×100 μm

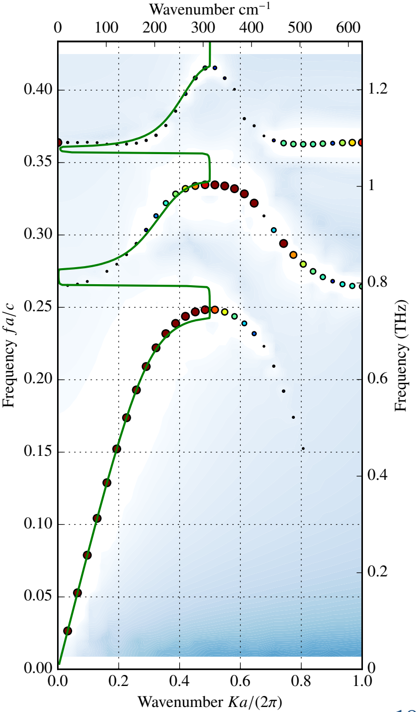

Current-driven homogenization (CDH) of an electro-magnetic split-ring resonator

inner capacitor radius of $\boldsymbol{\rho}_c = \mathbf{7}$ µm →

Bubbles are computed using CDH; the green dispersion curve comes from the scattering-parameters method. Note that

$$K = \frac{2\pi n f}{c}$$

capacitor splitting = 6 µm,
outer ring radius = 45 µm,
conductor cross-section = 10×10 µm
unit cell size = 100×100×100 µm

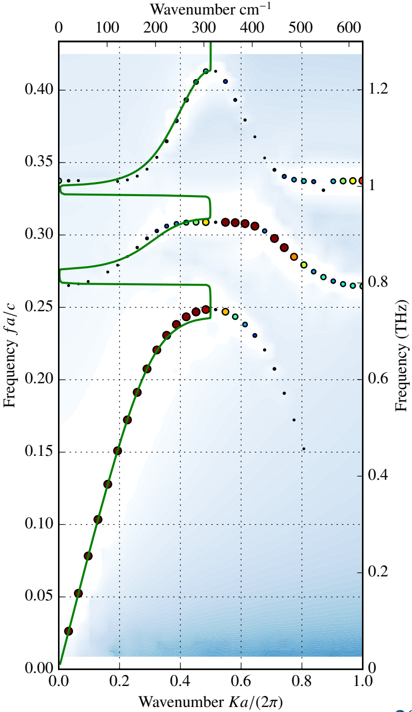

Current-driven homogenization (CDH) of an electro-magnetic split-ring resonator

inner capacitor radius of $\boldsymbol{\rho}_c = \mathbf{8}$ μm →

Bubbles are computed using CDH; the green dispersion curve comes from the scattering-parameters method. Note that

$$K = \frac{2\pi n f}{c}$$

capacitor splitting = 6 μm,
outer ring radius = 45 μm,
conductor cross-section = 10×10 μm
unit cell size = 100×100×100 μm

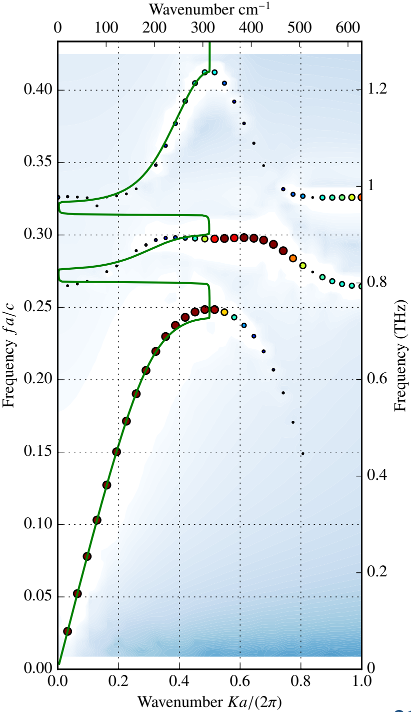

Current-driven homogenization (CDH) of an electro-magnetic split-ring resonator

inner capacitor radius of $\boldsymbol{\rho_c} = \mathbf{9}$ µm →

Bubbles are computed using CDH; the green dispersion curve comes from the scattering-parameters method. Note that

$$K = \frac{2\pi n f}{c}$$

capacitor splitting = 6 µm,
outer ring radius = 45 µm,
conductor cross-section = 10×10 µm
unit cell size = 100×100×100 µm

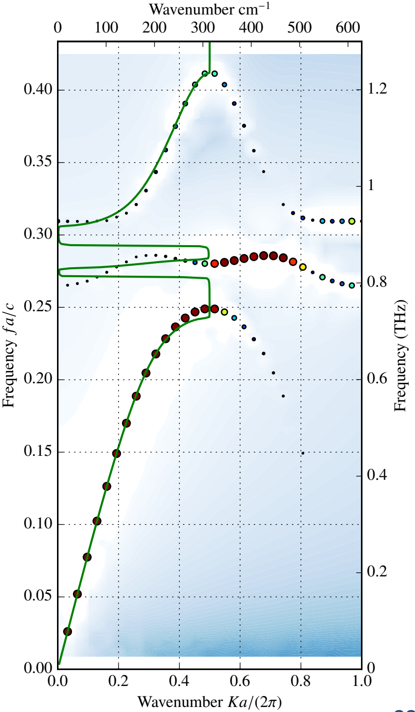

Current-driven homogenization (CDH) of an electro-magnetic split-ring resonator

inner capacitor radius of $\boldsymbol{\rho_c} = \mathbf{10}\ \mu\text{m} \rightarrow$

Bubbles are computed using CDH; the green dispersion curve comes from the scattering-parameters method. Note that

$$K = \frac{2\pi n f}{c}$$

capacitor splitting = 6 μm,
outer ring radius = 45 μm,
conductor cross-section = 10×10 μm
unit cell size = 100×100×100 μm

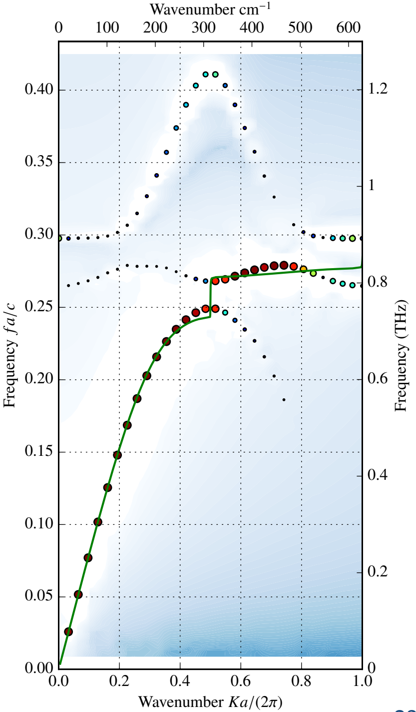

Current-driven homogenization (CDH) of an electro-magnetic split-ring resonator

inner capacitor radius of $\boldsymbol{\rho_c} = \mathbf{11}$ μm →

Bubbles are computed using CDH; the green dispersion curve comes from the scattering-parameters method. Note that

$$K = \frac{2\pi n f}{c}$$

capacitor splitting = 6 μm,
outer ring radius = 45 μm,
conductor cross-section = 10×10 μm
unit cell size = 100×100×100 μm

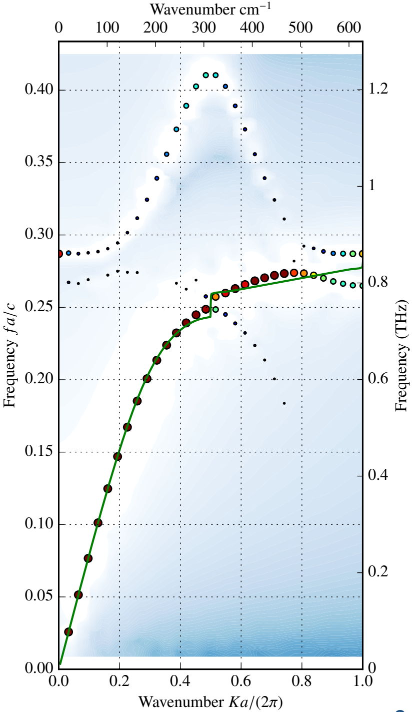

Current-driven homogenization (CDH) of an electro-magnetic split-ring resonator

inner capacitor radius of $\boldsymbol{\rho_c} = \mathbf{12}$ μm →

Bubbles are computed using CDH; the green dispersion curve comes from the scattering-parameters method. Note that

$$K = \frac{2\pi n f}{c}$$

capacitor splitting = 6 μm,
outer ring radius = 45 μm,
conductor cross-section = 10×10 μm
unit cell size = 100×100×100 μm

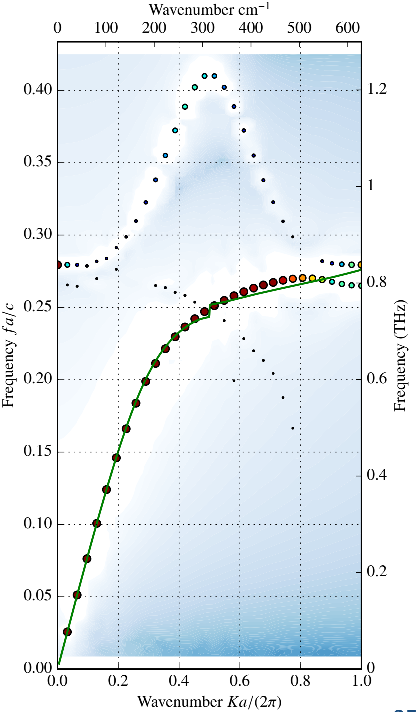

Current-driven homogenization (CDH) of an electro-magnetic split-ring resonator

inner capacitor radius of $\boldsymbol{\rho_c} = \mathbf{13}$ μm →

Bubbles are computed using CDH; the green dispersion curve comes from the scattering-parameters method. Note that

$$K = \frac{2\pi n f}{c}$$

capacitor splitting = 6 μm,
outer ring radius = 45 μm,
conductor cross-section = 10×10 μm
unit cell size = 100×100×100 μm

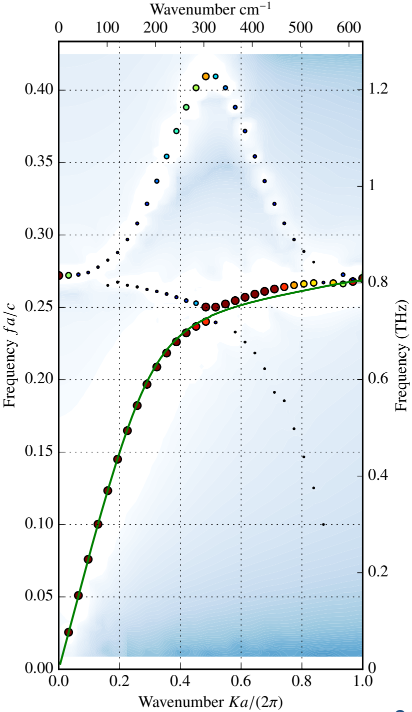

Current-driven homogenization (CDH) of an electro-magnetic split-ring resonator

inner capacitor radius of $\boldsymbol{\rho}_c = \mathbf{14}\ \mu\text{m} \rightarrow$

Bubbles are computed using CDH; the green dispersion curve comes from the scattering-parameters method. Note that

$$K = \frac{2\pi n f}{c}$$

capacitor splitting = 6 µm,
outer ring radius = 45 µm,
conductor cross-section = 10×10 µm
unit cell size = 100×100×100 µm

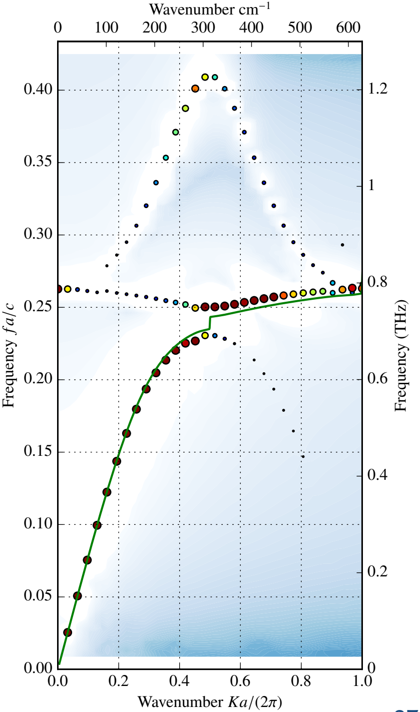

Current-driven homogenization (CDH) of an electro-magnetic split-ring resonator

inner capacitor radius of $\boldsymbol{\rho_c} = \mathbf{15}$ μm →

Bubbles are computed using CDH; the green dispersion curve comes from the scattering-parameters method. Note that

$$K = \frac{2\pi n f}{c}$$

capacitor splitting = 6 μm,
outer ring radius = 45 μm,
conductor cross-section = 10×10 μm
unit cell size = 100×100×100 μm

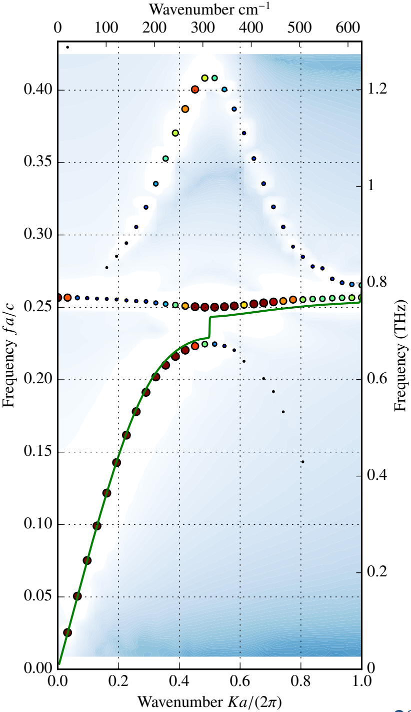

Current-driven homogenization (CDH) of an electro-magnetic split-ring resonator

inner capacitor radius of $\boldsymbol{\rho_c} = \mathbf{17}$ µm $\rightarrow$

Bubbles are computed using CDH; the green dispersion curve comes from the scattering-parameters method. Note that

$$K = \frac{2\pi n f}{c}$$

capacitor splitting = 6 µm,
outer ring radius = 45 µm,
conductor cross-section = 10×10 µm
unit cell size = 100×100×100 µm

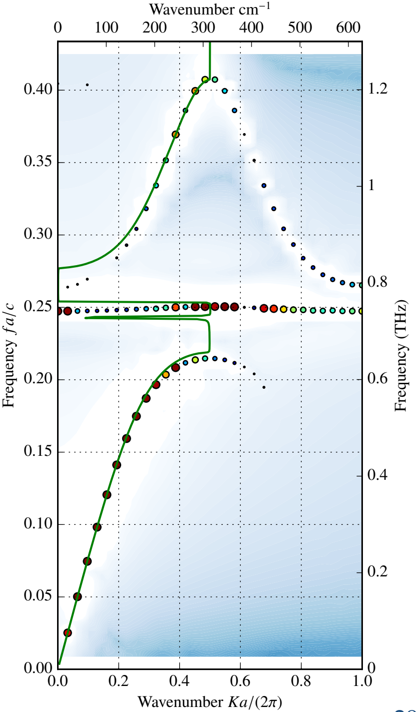

Current-driven homogenization (CDH) of an electro-magnetic split-ring resonator

inner capacitor radius of $\rho_c = \mathbf{18}$ µm →

Bubbles are computed using CDH; the green dispersion curve comes from the scattering-parameters method. Note that

$$K = \frac{2\pi n f}{c}$$

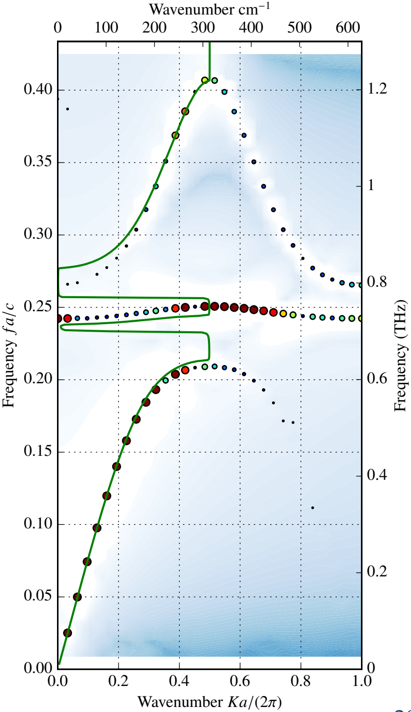

capacitor splitting = 6 µm,
outer ring radius = 45 µm,
conductor cross-section = 10×10 µm
unit cell size = 100×100×100 µm

- In the first part of the thesis I summed up relevant metamaterial theory, including topics that I felt to be underemphasized in the literature.
- I set up an environment for metamaterial simulation and homogenization, and I applied it to structures at the boundary between *metamaterials* and *photonic crystals*. I observed the customary scattering-parameters method to be more limited than is often perceived, and to fail e.g. when stronger spatial dispersion is present.
- A more reliable homogenization scheme (CDH) enabled me to compute the index of refraction for all structures under study.
- In the thesis, I documented the characteristics of ten basic classes of periodic structures, two of which were presented here.
- The simulation environment used is published at `https://github.com/FilipDominec/python-meep-utils`

- In the first part of the thesis I summed up relevant metamaterial theory, including topics that I felt to be underemphasized in the literature.
- I set up an environment for metamaterial simulation and homogenization, and I applied it to structures at the boundary between *metamaterials* and *photonic crystals*. I observed the customary scattering-parameters method to be more limited than is often perceived, and to fail e.g. when stronger spatial dispersion is present.
- A more reliable homogenization scheme (CDH) enabled me to compute the index of refraction for all structures under study.
- In the thesis, I documented the characteristics of ten basic classes of periodic structures, two of which were presented here.
- The simulation environment used is published at `https://github.com/FilipDominec/python-meep-utils`

Thank you for your attention!